Hindawi Publishing Corporation
Journal of Chemistry
Volume 2016, Article ID 1012021, 13 pages
http://dx.doi.org/10.1155/2016/1012021

Research Article

REE Geochemistry of Euphrates River, Turkey

Leyla Kalender and Gamze Aytimur

Department of Geological Engineering, Engineering Faculty, Fırat University, 23119 Elazığ, Turkey

Correspondence should be addressed to Leyla Kalender; leylakalender@firat.edu.tr

Received 3 March 2016; Revised 14 April 2016; Accepted 24 April 2016

Academic Editor: Stanislav Frančišković-Bilinski

The study area is located on the Euphrates River at 38°41′32.48″N–38°14′24.10″N latitude and 39°56′4.59″E–39°8′13.41″E longitude. The Euphrates is the longest river in Western Asia. The lithological units observed from the bottom to the top are Permo-Triassic Keban Metamorphites, Late Cretaceous Kömürhan Ophiolites, Upper Cretaceous Elazığ Magmatic Complex, Middle Eocene Maden Complex and Kırkgeçit Formation, Upper Pliocene and Lower Eocene Seske Formation and Upper Miocene, Pliocene Karabakır and Çaybağı Formations, Palu Formation, and Holocene Euphrates River sediments. The geochemical studies show that $^{87}Sr/^{86}Sr$ and $^{143}Nd/^{144}Nd$ isotopic compositions in the Euphrates River bank sediments are 0.7053, 0.7048, and 0.7057 and 0.512654, 0.512836, and 0.512775, respectively. These values indicate mixing of both carbonate-rich shallow marine sediment and felsic-mafic rocks from Elazığ Magmatic Complex into the stream sediments. The positive $\varepsilon Nd(0)$ values (0.35, 3.9, and 2.7) are higher downstream in the studied sediments due to weathering of the mafic volcanic rocks. The chondrite, NAS, and UCC normalized patterns show that the REE compositions of the Euphrates River sediments are higher than chondrite composition but close to NAS and UCC. The river sediments in the tectonic zone and the weathered granodioritic rocks of the Elazığ Magmatic complex affect upstream water compositions.

1. Introduction

A number of researchers have studied Nd-Sr isotopic and trace element geochemistry of river sediments and soils as tracers of clastic sources. The geochemical characterizations and Sr-Nd isotopic fingerprinting of sediments in any fluvial system can be done using radiogenic isotopic compositions [1–5]. Rare earth elements (REEs) compositions have been studied in stream sediments [6–8] and in chemical weathering of drainage systems [9–12]. A number of researchers have studied REE composition of both river sediments and river water and discovered that heavy REE concentration is higher in the river sediments than in suspended matter in river water. They also indicated that shale, Upper Continental Crust, and chondrite normalized REE patterns showed that chemical weathering from source rocks in the continental crust, erosion, and terrigenous fluviatile sediment sources can be distinguished using the REE compositions of rivers [13–18]. Leybourne et al. [19] indicated that Ce and Eu can be redox sensitive and attributed to determination of redox conditions. Yang et al. [8] stated that source rock composition is a more important factor affecting REE composition than weathering processes. There are fewer studies on the Euphrates River. Kalender and Bölücek [20] studied the stream sediments in the north Keban Dam Lake in the Eastern Anatolian district and demonstrated that more REEs are transported with Fe and Mn rich oxides and fine size fraction sediments (e.g., clay minerals) via adsorption. Kalender and Çiçek Uçar [21] indicated that the calculated enrichment factor values of the heavy REE are more than those of light REE in the Geli stream sediments. Geli stream is a tributary of the Euphrates River. Rivers carry the weathered rock products from the continents to the dam lakes, natural lakes, and the sea. Thus, this study focuses on the REE concentrations in river bank sediments from the initial point of the Euphrates River (10 kilometers upstream of Keban Dam) to Karakaya Dam Lake. In order to evaluate distribution of REE along the flowing direction of the Euphrates River, the sediment sources and lithological controls were identified using Upper Continental Crust (UCC), North American Shale (NAS), and Chondrite (Ch) normalized REE patterns (all average values taken from [8, 22–25]). Goldstein and Jacobsen [13] studied

REE compositions in river water, and major rivers have LREE enriched patterns relative to the NAS, and negative Ce anomalies occur at high pH. This paper firstly presents REE concentrations and includes source rock composition of the Euphrates River sediments and waters.

2. Geology

The Euphrates River is located in the Eastern Anatolian district in Turkey and is located on the active tectonic zone of the East Anatolian fault zone. The East Anatolian fault zone is seismically one of the most active regions in the world and is located within the Mediterranean Earthquake Zone, which is a complicated deformation area that was formed by the continental collision between the African-Arabian and Eurasian continents. These deformations involve thrust faults, suture zones, and active strike slip and normal faults, as well as basin formations arising from these faults. The Euphrates River is located on the East Anatolian fault zone and is formed by the mixing of the Karasu River and Murat River 10 kilometers upstream of the Keban Dam. According to Frenken [27], the Euphrates River length is 1100 km from Palu to the Red Sea (Figures 1(a) and 1(b)). The studied sediments were sampled along approximately 50 kilometers of the Euphrates River length. The main stratigraphic units found in the Euphrates River basin range from the Permo-Triassic Keban Metamorphites to Plio-Quaternary Palu Formation (Figure 1(b)). The Keban Metamorphites outcrop on both right and left banks of the Euphrates River. Considering the regional scale, the Keban Metamorphites are represented by marble, recrystallized limestone, calc-schist, metaconglomerate, and calc-phyllite in the study area [28]. Additionally, in the study area, the Upper Cretaceous Elazığ Magmatic Complex consists of volcanic rocks (basalt, andesite, pillow lava, dacite, and volcanic breccia), subvolcanic rocks (aplite, microdiorite, and dolerite), and plutonic rocks (diorite, tonalite, granodiorite, granite, and monzonite). The magmatic rocks are overlain by recrystallized limestone of the Permo-Triassic Keban Metamorphites [29]. The Late Cretaceous Kömürhan Ophiolites are part of the southeast Anatolian ophiolite belt which are formed in a suprasubduction zone within the southern Neo-Tethys [30]. The Kömürhan Ophiolites consist of dunite, layered and isotropic gabbros, plagiogranite, sheet dyke complex, andesitic and basaltic rocks, and volcanosedimentary rocks. The unit is observed in the Karakaya Dam Lake area (Figure 1(b)). Upper Paleocene and Lower Eocene massive limestones are named the Seske Formation which is characterized by interbedded clastic and carbonate rocks. The stratigraphic position of the Seske Formation indicates the extent of how Neo-Tethys was controlled by the tectonic and topographic features of the region during the Eocene [31, 32]. The Seske Formation is observed along the Karakaya Dam Lake (Figure 1(b)). Middle Eocene Maden Complex is composed of basaltic and andesitic rocks and limestone, conglomerates, sandstones, and mudrocks (marl) [29, 33–35]. Middle Eocene Kırkgeçit Formation consists of marine conglomerates, marls, and limestone from the bottom to the top [36]. The Alibonca Formation was deposited after closure of the Neo-Tethys Ocean in Mesozoic time. The unit is composed of sandy limestone and marls which are observed in the Keban Dam Lake area [37] (Figure 1(b)). Upper Miocene-Pliocene Karabakır and Çaybağı Formations consist of sandstone, mudrock, marls, tuff, and basaltic rocks [36]. The units are observed in the northeast of the Keban Dam Lake (Figure 1(b)). The Çaybağı Formation is named by Türkmen [38] at the Çaybağı township in the east of Elazığ. Pliocene-Quaternary units are named the Palu Formation by Kerey and Türkmen [39]. The units consist of quaternary alluvial and fluvial deposits along the level bank of the Murat River which is the initial point of the Euphrates River (Figures 1(a) and 1(b)).

3. Analytical Methods

3.1. Climatic Information. Maximum flows of the Euphrates River occurred from February through April, whereas minimum flows occurred from August through October. The annual mean rainfall during that period was 372 mm, and the air temperature varied between 15.21°C (Elazığ) and 16.31°C (Malatya) with the highest and the lowest temperature of 34°C and minus 10, respectively, between 1992 and 2001. The continental climate of the Euphrates Basin is a subtropical plateau climate (data was taken from reports by the Elazığ Meteorology Department). The Euphrates River sediment samples were collected in September, the period of minimum flow of the Euphrates River water. It is also good to take into consideration the effect on chemical compositions of the river bed sediment of processes erosion of the earth's surface. The sediment samples were taken from locations close to the center of the river bed in consideration of the erosional process and chemical composition of the river bed sediments.

3.2. Sampling Sites. In this study, directing studies could not be performed in advance of the development of sample taking methods and suitable particle size and chemical analysis methods. Ninety river sediments and water samples were taken from the right side of the river bed along the direction of the river water flow because it is suitable for sampling of river bed morphology (Figure 1(b)).

3.3. Sample Preparing for Analysis. The samples were taken in September, when the water flow rate was low. In order to prevent the existence of particles in the sediment samples that were too large, the samples were sifted through sieve with hole diameter of 2 mm (BS10 mesh) so as to obtain the suitable particle sizes. 2 Kg of the river sediment samples was taken at 250–500 m intervals along the Euphrates River (from 10 kilometers upstream of the Keban Dam to Karakaya Dam, 50 kilometers) and placed into plastic bags, numbered, and dried at room temperature. After drying, the samples were sifted to different sieve dimensions in order to determine the particle size fractions suitable for analysis (−200 mesh). In the study of some metals and REE concentrations in sediments, many researchers prefer the grain size of fine-medium sand to silt (−74 μm) as it shows very high concentrations, higher than −80 mesh (−180 μm) [8, 21, 40, 41]. In order to minimize the grain size dependencies of heavy metals, concentrations of −75 μm fraction, representing medium fine sand to silt,

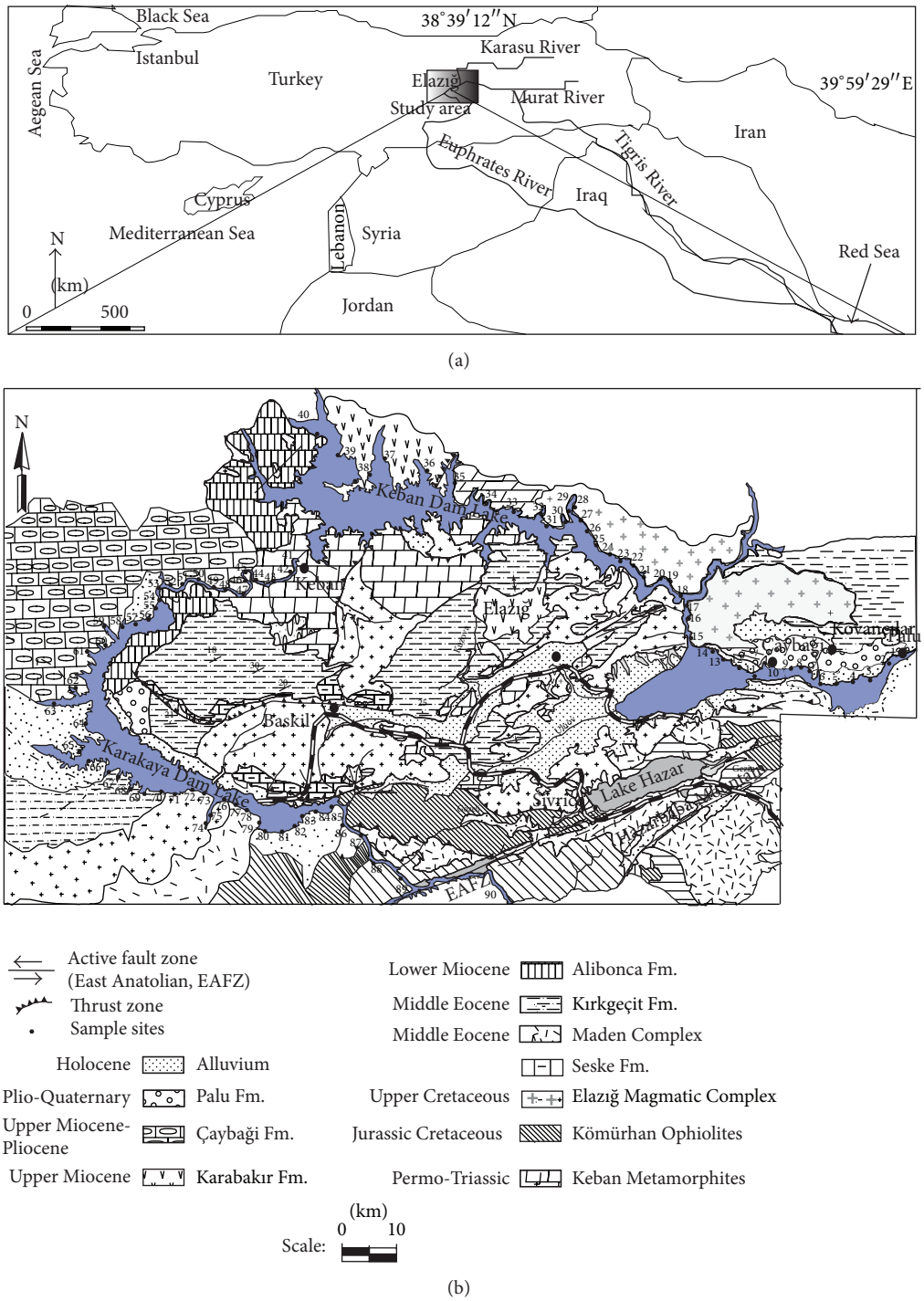

Figure 1: (a) Location map. (b) Geology map of the Euphrates River and the sampling sites (from 1 to 90, the geology map was modified from Herece et al. [26]).

were used in the present study. Mechanical wet sieving was performed to separate the −74 μm sediment fraction from the bulk samples. Fifteen to twenty grams of each sample was freeze dried for 8 and 9 hours. The sieved fractions were placed in clean porcelain bowls and dried at room temperature.

3.4. Chemical Analysis. Elazığ Magmatic Complex includes zirconium- and titanium-bearing minerals [30]. As commonly known, zirconium- and titanium-bearing minerals contain amounts of REE. This method was preferred due to its convenience for the decomposition of the silicate minerals using HF. HF is an efficient disintegration agent

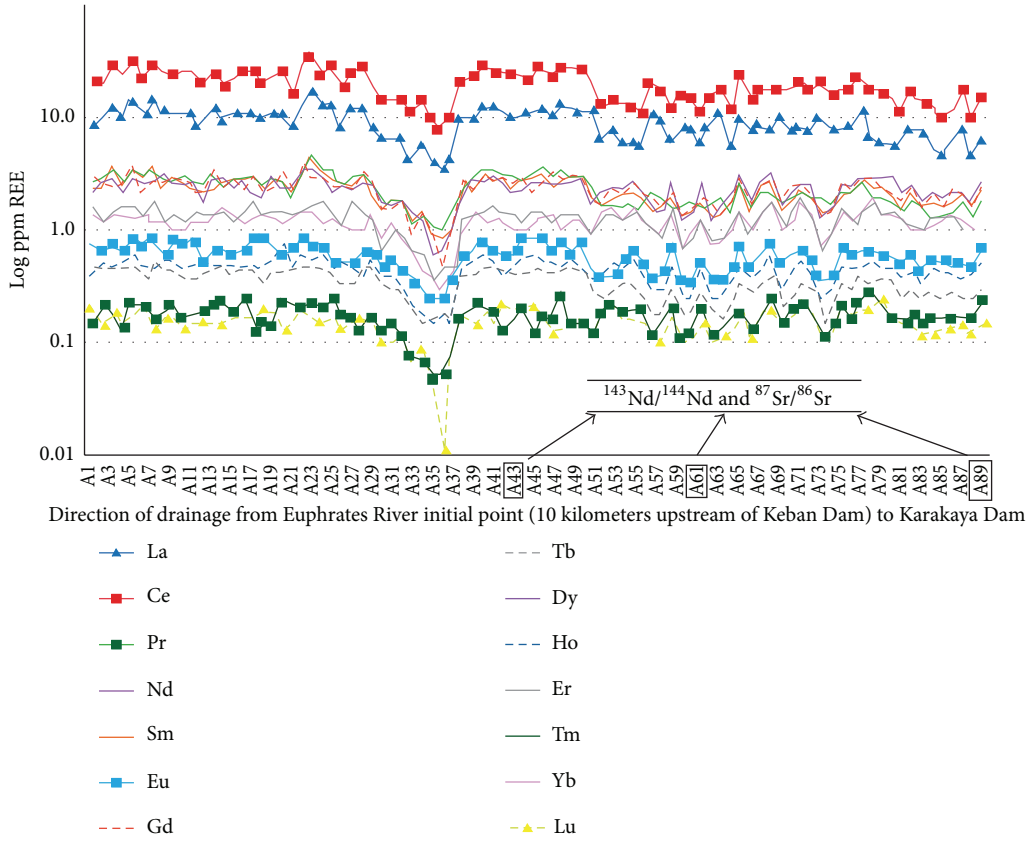

FIGURE 2: Distribution of REE and the determined sample sites (A43, A61, and A89) for ^{87}Sr/^{86}Sr and ^{143}Nd/^{144}Nd isotopic analysis from the Euphrates River sediments.

used for the decomposition of zirconium silicate and apatite source from granitoids in nature. This decomposition method causes the loss of silica as SiF_4 and a part of titanium as TiF_4. Bulk samples were ground and sieved through 200-mesh (about 0.074 mm pore size) stainless steel sieve for chemical analysis. 0.5 g of each sediment sample was leached with 90 mL HCl-HNO_3-HF at 95°C for 1 hour, diluted to 150 mL, and then analyzed by ICP-OES. The extraction method used by Saito et al. [42] was used to obtain the maximum REE concentration at 9.95 mL 0.01–1 m nitric acid aqueous solution (pH < 4). Standard DS5 was used for the sediment analyses. The sediment samples were analyzed for REE in Acme Analytical Laboratories Ltd., Canada, by Inductively Coupled Plasma-Optical Emission Spectrometer (ICP-OES). The river water samples have less than 0.1% total dissolved solids, and these analyses were used by ICP-OES at Bureau Veritas environmental lab, Maxxam Analytics. The isotopic measurements were made at the Middle East Technical University (Ankara, Turkey) following the protocol of Köksal and Göncüoğlu [43]. TLM-ARG-RIL-02 methods were adopted. An 80 mg aliquot was taken for analysis of Sr and Nd isotope ratios. The samples were dissolved in beakers in a 4 mL 52% HF at 160°C on the hotplate along four days. The samples were dried on the hotplate using 2.5 N HCl and 2 mL bis(ethylhexyl) phosphate using Bio-Rad AG50 W-X8, 100–200 mesh, and chemical seperation of Sr ionic chromatographic columns was prepared. After chemical separation of Sr, REE fractionation was collected using 6 N HCl. Sr isotopes were measured using a single Ta-activator with Re filament and 0.005 N H_3PO_4 [44]. ^{87}Sr/^{86}Sr ratios were corrected for mass fractionation by normalizing to ^{86}Sr/^{88}Sr = 0.1194, and strontium standard (NBS 987) was measured more than 2 times. The chemical separation of Nd from REE was made in a teflon column using 0.22 N HCl and 2 mL bis(ethylhexyl) phosphate. ^{143}Nd/^{144}Nd data were normalized by ^{146}Nd/^{144}Nd = 0.7219, and neodymium standard (0.511848 ± 5) was measured more than 2 times.

4. Results

4.1. Nd-Sr Isotope Compositions of the Euphrates River Sediments. REE concentrations of the Euphrates River sediments from Keban Dam to Karakaya Dam are presented in Table 1. The result of isotopic composition of the studied sediments and those from different origin, summarized statistical values, and REE compositions of the Mississippi and Amazon River sediments are presented in Table 1. The 75 μm (200 mesh) size fraction from the Euphrates River sediment samples (A43, A61, and A89) was analyzed for ^{87}Sr/^{86}Sr and ^{143}Nd/^{144}Nd ratios (Figure 2 and Table 1). The study shows that ^{87}Sr/^{86}Sr and ^{143}Nd/^{144}Nd isotopic compositions have range of 0.7053, 0.7048, and 0.7057 and 0.512654, 0.512836,

Table 1: Summary statistical values of REE from Euphrates River sediments. Density values (g/cm^3) taken from Gupta and Krishnamurthy [45]. *Sediments from Sholkovitz [46]. Calculated εNd and 1000/Sr data from Martin and McCulloch [4]; **Burke et al. [1]; ***Bussy [2]; ****Akgül et al. [47], +Mensel et al. [48].

(a)

LREE $N = 90$	Density	Max./min. values	Euphrates River (ppm)	*Mississippi River	*Amazon River	HREE $N = 90$	Density	Max./min. values	Euphrates River (ppm)	*Mississippi River	*Amazon River
La	6.14	3.4/15.9	8.57	60.8	349	Tb	8.23	0.18/0.47	0.33	—	—
Ce	8.16	7.5/34.4	18.11	125.4	707	Dy	8.55	0.63/3.12	2.17	7.46	39.7
Pr	6.77	0.88/4.46	2.22	—	—	Ho	8.79	0.17/0.63	0.43	—	—
Nd	7.00	5.39/12.1	7.70	56.4	355	Er	9.06	0.43/1.67	1.20	4.94	21.7
Sm	7.52	0.82/4.05	2.14	—	—	Tm	9.32	0.05/0.28	0.17	—	—
Eu	5.24	0.23/0.82	0.57	2.11	10.9	Yb	6.96	0.29/1.59	1.11	3.94	20.5
Gd	7.90	0.44/3.65	2.20	9.86	46.3	Lu	9.84	0.02/0.23	0.15	0.47	3.02
Mean			5.93	—	—	Mean			0.79	—	—
St. deviation			6.18	—	—	St. deviation			0.74	—	—

(b)

The result of isotopic composition of the studied sediments and some examples in the world				
Sample code	$^{143}Nd/^{144}Nd$	$^{87}Sr/^{86}Sr$	εNd (0)	1000/Sr
A43	0.512654	0.7053	0.35	16.1
A61	0.512836	0.7048	3.9	13.74
A89	0.512775	0.7057	2.7	13.17
Basaltic soil+	0.511783	0.705603	2.26	3.9
Metased. soil+	0.512501	0.709646	−2.67	6.57
Metagreywackes+	0.512847	0.705374	4.08	2.49
Sediments+	0.512805	0.704583	3.26	4.0
**Jurassic-Cretaceous sediments	—	0.707–0.708	—	—
***Arve River sediments	—	0.728	—	Related to Mont-Blanc granite
		0.704	—	Carbonate-rich rocks
****Elazığ Magmatites Upper Cretaceous	0.512414–0.512851	0.706022–0.708451	7.5	Diorites and —
			3.5	granites —

and 0.512775, respectively. εNd (0) values were calculated using

$$\varepsilon\mathrm{Nd}\,(0) = \frac{^{143}\mathrm{Nd}/^{144}\mathrm{Nd}\ (\mathrm{Measured})}{0.512636} - 1 \times 10^4 \qquad (1)$$

(see [48, 49]).

The calculated εNd (0) values have range of 0.35, 3.9, and 2.7. Table 1 shows the result of the radiogenic isotope compositions in the Euphrates River sediments, $^{87}Sr/^{86}Sr$ and $^{143}Nd/^{144}Nd$, and calculated εNd (0) data of the sediments from different origins. The isotope compositions ratios of $^{143}Nd/^{144}Nd$ and $^{87}Sr/^{86}Sr$ in the Euphrates River sediments suggest that the REE pattern of river sediments changes systematically with the compositions of the rocks in the drainage area. The range of $^{87}Sr/^{86}Sr$ ratios found in the Euphrates River sediments may be explained using metagreywackes and sediments (0.705374, 0.704835, and 0.704583, resp.) according to Table 1. The calculated 1000/Sr ratios are 16.1 (A43), 13.17 (A61), and 13.74 (A89), and Nd values are 5.98 (A43), 6.45 (A61), and 8.40 (A89) ppm, while La concentrations are 9.8 (A43), 7.8 (A61), and 4.5 (A89) ppm. The comparison with 1000/Sr and La values indicated that the weathering of felsic igneous rocks decreases downstream of the Euphrates River, while it increases in the mafic igneous rocks.

4.2. REE Results of the Euphrates River Sediments. Large variations are observed in the distribution of the REE in the Euphrates River sediments (Table 1). La concentrations range from 3.4 to 15.9 ppm, while Lu concentrations range from 0.02 to 0.23 ppm. The concentrations of the light REE are 7.5 times higher than heavy REE concentrations. Ce concentrations range from 7.5 to 34.4 ppm. Figure 2 plots indicate that the concentrations of La and Ce are the highest along the flowing direction of the Euphrates River. The concentrations of the REE at the A37 sample site decrease because of the next thrust zone. Thus, the circulation of mixing waters possibly influenced the concentrations of REE in the studied river sediments. The REE plots for the Euphrates River sediments in this study exhibit a small degree of variation. The abundance of the REE in the river sediments is probably due to the mineralogic characterizations of the regional rocks. Figure 2 plots can be explained to mean that the variations of the light REE along the flowing direction are higher until A51 sample site, except for A34, A35, A36, and A37 sites. The heavy REE concentrations increase from A51 sample site to A90 because of the mineralogic characterizations of mafic volcanic and metaophiolitic rocks.

4.3. REE Results of the Euphrates River Water. REE concentrations of the Euphrates River waters are presented in Table 3. The Amazon, Indus, Mississippi, and Ohio Rivers water data from Goldstein and Jacobsen [13] are also presented in Table 3. La concentrations have range from 0.02 to 2.63 ppb, and Ce concentrations have range from 0.12 to 5.43 ppb. The highest Ce and La values in the water samples are observed at the A34 site, and Pr, Sm, Gd, Dy, Er, and Yb have the highest values, 0.07, 0.07, 0.07, 0.06, 0.03, and 0.03 ppb, respectively, at the same site. However, the lowest Ce and La concentrations in the studied sediments were observed at the same site. The results indicate that the circulation of mixing water along the tectonic zones can be a much more important factor on the absolute abundance of the REE in river sediments than weathering of the regional rocks.

5. Discussion

The results suggest that the tectonic zone is an important factor in controlling the abundance of the REE concentrations in the Euphrates River sediments. Moreover, the study indicates that the REE compositions are dependent upon the type (subtropical climatic influences, water circulation, riverbed morphology, and secular variation) of weathered regional rocks. The comparison of $^{87}Sr/^{86}Sr$ compositions of the Euphrates River sediments with those from basaltic soil and metasedimentary soil from Sholkovitz [46] in Table 1 shows that the studied sediments have basaltic and metagreywackes characterization (Figure 3). Bussy [2] obtained 0.728 for $^{87}Sr/^{86}Sr$ ratio in the Arve River sediments which are related to the Mont-Blanc granites (Table 1). However, this study reveals that $^{87}Sr/^{86}Sr$ ratio in carbonate-rich rocks is 0.704. The lower $^{87}Sr/^{86}Sr$ ratios (0.7053, 0.7048, and 0.7057 obtained for the sample sites A43, A61, and A89, resp.) from river sediments in the Keban Dam Lake area, downstream of the contact between the Permo-Triassic shallow marine metasediments and the Upper Cretaceous magmatic crystalline complex of the Elazığ Magmatic Complex, are caused by mixing of the two sources. $^{143}Nd/^{144}Nd$ isotopic compositions in the studied river sediments determined have range values of 0.512650, 51283640, and 512775 (Table 1), and the values are similar to the composition of metagreywackes. $^{143}Nd/^{144}Nd$ isotopic composition ratios have range values 0.512414 to 0.512851 for granodiorites in Upper Cretaceous Elazığ Magmatites [47] (Table 1). These comparisons indicate that the weathered felsic igneous rocks in the river sediments are greater at the A43 sample site because of Upper Cretaceous granitic rocks from Elazığ Magmatic Complex than at the A61 and A89 sample sites. These sites have weathered basaltic igneous rocks compositions due to Upper Cretaceous basic volcanic rocks of the Elazığ Magmatic Complex. Figure 3 shows that neodymium isotope ratios in the New England fold belt change from positive εNd (0) values in tertiary basalt to negative values in granitoids and metapelitic rocks [48]. The positive εNd (0) values reflected the contribution of the isotope compositions in the downstream sediments due to weathering of the basic volcanic rocks. Thus, regional and local studies indicate that the Euphrates River sediments have different isotope composition due to mixing of different weathered source rocks (e.g., Permo-Triassic Keban Metamorphites and Upper Cretaceous Elazığ Magmatic Complex, granodioritic and basic volcanic rocks). The Euphrates River sediments have the lowest average REE concentrations, while the Mississippi and Amazon River sediments yield the highest values. Table 1 shows that the average LREE (La, Ce, Nd, Eu, and Gd) and HREE (Dy, Er, Yb, and Lu) compositions of the Euphrates River sediments

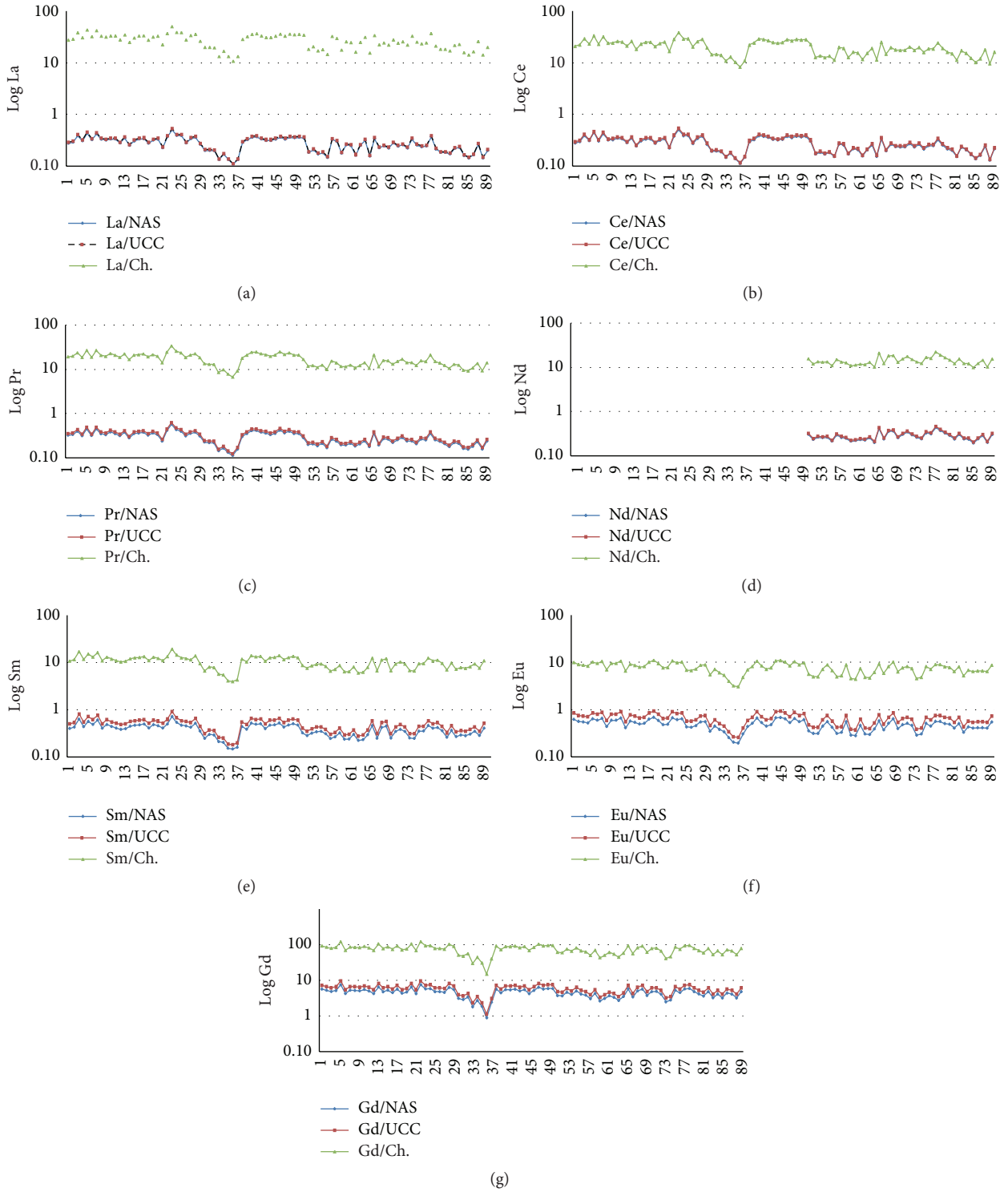

FIGURE 3: Normalized patterns of the LREE average concentrations ($N = 90$) of Euphrates River sediments in the NAS, UCC, and Ch. (a) La, (b) Ce, (c) Pr, (d) Nd* ($N = 50$), (e) Sm, (f) Eu, and (g) Gd normalized patterns.

are lower by 8.33 to 3.63 and 39.52 to 18.34 times compared to the REE compositions of the Mississippi River and Amazon River REE compositions. The researchers indicated that the light and middle REE enrichment in river sediments may be related to apatite-rich rocks [52, 53]. However, Kalender and Çiçek Uçar [21] suggested that the calculated enrichment factor values of the heavy REE are more than those for the light REE in the tributaries of the Euphrates River sediments

Table 2: North American Shale (NAS), upper continental crust (UCC), and chondrite (Ch.) from Yang et al. [8], Condie [22], Taylor et al. [23], and Sholkovitz [50, 51] and normalized REE summary statistical values (ppm) in Euphrates River sediments; *Obaje et al. [18].

LREE	Mean	St. dev.	*Nigerian Gora River	HREE	Mean	St. dev.	*Nigerian Gora River
La/NAS	0.28	0.08	—	Tb/NAS	0.39	0.11	—
La/UCC	0.29	0.09	—	Tb/UCC	0.52	0.15	—
La/Ch.	**26.77**	8.08	39.76	Tb/Ch.	**6.51**	1.85	—
Ce/NAS	0.27	0.09	—	Dy/NAS	0.52	0.13	—
Ce/UCC	0.28	0.09	—	Dy/UCC	0.62	0.15	—
Ce/Ch.	**20.12**	6.34	**17.96**	Dy/Ch.	**7.23**	1.78	—
Pr/NAS	0.29	0.09	—	Ho/NAS	0.42	0.10	—
Pr/UCC	0.31	0.10	—	Ho/UCC	0.53	0.13	—
Pr/Ch.	**17.10**	5.46	—	Ho/Ch.	**5.74**	1.41	—
Nd/NAS	0.28	0.06	—	Er/NAS	0.42	0.10	—
Nd/UCC	0.30	0.06	—	Er/UCC	0.52	0.13	—
Nd/Ch.	**14.26**	2.97	18.96	Er/Ch.	**5.73**	1.39	—
Sm/NAS	0.38	0.11	—	Tm/NAS	0.35	0.09	—
Sm/UCC	0.48	0.14	—	Tm/UCC	0.51	0.14	—
Sm/Ch.	**10.20**	3.00	—	Tm/Ch.	**5.22**	1.41	—
Eu/NAS	0.48	0.12	—	Yb/NAS	0.36	0.09	—
Eu/UCC	0.65	0.17	—	Yb/UCC	0.51	0.12	—
Eu/Ch.	**7.70**	1.98	404.62	Yb/Ch.	**6.18**	1.47	25.52
Gd/NAS	0.45	0.12	—	Lu/NAS	0.33	0.09	—
Gd/UCC	0.58	0.16	—	Lu/UCC	0.47	0.12	—
Gd/Ch.	**7.35**	1.98	58.50	Lu/Ch.	**4.68**	1.23	—

Table 3: REE concentrations in river water in ppb. The Amazon, Indus, Mississippi, and Ohio Rivers data from Goldstein and Jacobsen [13].

LREE $N = 90$	River water	Dissolved load			
	Euphrates	Amazon	Indus	Mississippi	Ohio
La	0.25	0.074	0.0029	0.020	0.0063
Ce	0.54	0.21	0.0024	0.010	0.010
Pr	0.04	—	—	—	—
Nd	0.18	0.13	0.0032	0.020	0.011
Sm	0.04	0.034	0.00071	0.004	0.0025
Eu	<0.01	0.008	0.00022	0.001	0.0006
Gd	0.04	—	0.050	—	—
Tb	<0.01	—	—	—	—
Dy	0.04	0.031	0.036	0.0075	0.006
Ho	<0.01	—	—	—	—
Er	0.02	0.016	0.017	0.0065	0.005
Tm	<0.01	—		—	—
Yb	0.2	0.015	0.0014	—	0.0036
Lu	<0.01	—	0.0021	—	0.0006

due to Fe-Mn oxyhydroxide adsorption capacity for HREE linked to the basic volcanic rocks source of HREE. Yang et al. [8] stated that zircon contributes to the bulk HREEs in sediments because of the relatively high abundance of HREEs in zircon. The lithologic units along the Euphrates River bed contribute to the bulk of LREEs concentrations as a result of apatite-rich, zircon-poor Upper Cretaceous granodiorites. La/Yb mean ratio of 7.72 in the studied sediment samples indicated high erosional rate because La may be removed from crustal source via weathering process and this is in agreement with the finding of Obaje et al. [18]. The distribution trend of REE along the flowing direction of the Euphrates River at some of the sample locations A32, A33, A34, A35, and A36 indicates that the thrust zone between Upper Cretaceous Elazığ Magmatic Complex and Permo-Triassic Keban Metamorphites influences the decreasing REE composition in the river sediments due to mixing water circulation. Average LREE concentrations upstream have higher-than-average HREE concentration compared to downstream ones due to the shallow marine metasediments and felsic magmatic rocks (Permo-Triassic Keban Metamorphites, felsic rocks from Upper Cretaceous Elazığ Magmatites) upstream. However, the basic volcanic rocks (Maden Complex and Kömürhan metaophiolites) are observed downstream along the Euphrates River flowing direction. Obaje et al. [18] and Ramesh et al. [54] stated that positive Ce anomalies are related to the formation of Ce^{4+} and Ce hydroxides and terrigenous input and diagenetic conditions. The positive Ce anomalies may indicate hydromorphic distribution of the REE in river sediments. According to some researchers, Eu anomalies have less contribution from felsic magmatic rock weathering. The negative Eu anomalies (<0.01 detection limit) indicate that the REE compositions in the river sediments more or less contribute to felsic magmatic rock weathering compared with terrigenous input and basic magmatic rock weathering. Lower river flowing velocity may

be responsible for REE homogenous REE distribution in agreement with Obaje et al. [18]. The average chondrite normalized values indicate LREE and HREE enrichment, and their summarized statistical values range from 26.77 to 7.35 and 7.23 to 4.68, respectively (Table 2). The chondrite normalized patterns illustrate that the REE composition of the Euphrates River sediments differs from chondrite composition but also the REE enrichment is close to NAS and UCC. The REE normalized values of the Nigerian Gora River from Obaje et al. [18] are shown in Table 3. The Ce/Ch. value is higher (20.15) in the Euphrates River sediments than the Nigerian Gora River sediments (17.96) due to sulfide-rich mineralization in the studied area, especially Keban polymetallic mine deposit. Ramesh et al. [54] revealed that the positive Ce anomalies indicate terrigenous input, depositional environment, and diagenetic conditions due to the formation of Ce^{4+} and stable Ce hydroxides. According to Nielsen et al. [55], Tl and Ce may be controlled by residual sulfide and clinopyroxene, respectively, during mantle melting due to their highly different ionic charges and radii. Luo et al. [56] indicated that while the adsorption ability of REE decreases on colloidal particles from light (La) to heavy (Lu), the complexes of REE with carbonate increase, and also the larger colloidal particles have stronger ability to adsorb Ce from weathering of granitic rocks. However, both LREE and HREE concentrations are lower than NAS and UCC (Figures 4 and 5). LREE patterns show that Sm and Eu patterns are closer to 1, and Gd pattern is higher than 1 La, Ce, Pr, and Nd (Figures 4(a), 4(b), 4(c), 4(d), 4(e), 4(f), and 4(g)). $Gd/Yb_{NAS\ and\ UCC}$ ratio >1 indicates that apatite from granodioritic rocks had contributed to the river sediment REE compositions [57–61]. According to Leybourne and Johannesson [60], Eu is mobilized during hydromorphic transport compared to Sm and Gd. However, the study reveals that Sm and Eu are mobilized more compared to Gd. Thus, Gd enrichment was observed in the river sediments. However, HREE patterns enrichment is relative to chondrite but HREE NAS and UCC normalized patterns are observed to be close to 1 (Figures 5(a), 5(b), 5(c), 5(d), 5(e), 5(f), and 5(g)). All of the river sediment REE compositions that display enrichment are relative to chondrite REE composition.

REE compositions of the Euphrates River water were compared with REE in dissolved load of Amazon, Indus, Mississippi, and Ohio River waters from Goldstein and Jacobsen [13] (Table 3). Figure 6 indicates that the REE compositions of the Euphrates River water are higher than REE compositions in the dissolved load compared of the Amazon, Indus, Mississippi, and Ohio Rivers. However, the REE patterns of the Euphrates River water were similar to REE in dissolved load in the Amazon, Indus, Mississippi, and Ohio River waters. Yb content in the Indus River water is higher while Ce content in the Mississippi River water is lower than in the Euphrates River water. According to Goldstein and Jacobsen [13], high Yb values in suspended materials may be derived from older rocks. Goldberg et al. [62] indicated that Ce depletion in river waters in a high pH environment may be related to the result of preferential removal of Ce^{4+} onto Fe-Mn oxide coatings of particles. This indicates that suspended materials load in the Euphrates River water is probably more than in the Mississippi, Ohio, and Indus River waters. Ce anomalies are calculated using the following equation:

$$Ce^{*} = \frac{3Ce_{NAS}}{\left(2La_{NAS} + Nd_{NAS}\right)} \quad (2)$$

from [13], where

$$Ce^{*} = 3 \times 0{,}000024\,(2 \times 0.000015 + 0{,}000020) = 1.16. \quad (3)$$

As shown, positive Ce anomalies ($Ce^{*} > 1$) support the fact that Ce may be fixed on the clay at pH > 7. Also, the calculated $(La/Yb)_{NAS}$ values in the Euphrates River water and sediment are 0.098 and 0.77. It is apparent that both Euphrates River waters and sediments have heavier REE composition than light REE according to NAS normalized patterns.

6. Conclusions

(1) This paper indicates that a contribution from a third component can change the isotopic composition of the studied sediments: (a) Permo-Triassic carbonate-rich metasediments and (b) felsic magmatic and (c) mafic volcanic rocks from Upper Cretaceous Elazığ Magmatic Complex.

(2) The study indicates that the Euphrates River average LREE (La, Ce, Nd, Eu, and Gd) and HREE (Dy, Er, Yb, and Lu) compositions have lower range values from 8.33 to 3.63 and 39.52 to 18.34 times less than Mississippi River REE and Amazon River sediment compositions, respectively.

(3) This paper revealed that the Euphrates River has higher LREE than HREE concentrations, and also, in the thrust zone which is close to the Euphrates River bed, there is low REE composition due to fast water circulation.

(4) Average LREE concentrations upstream in the Euphrates River are higher than average HREE concentrations downstream due to felsic magmatic rocks.

(5) La/Yb ratio (7.72) indicates high erosion rate, and La may have been added from crustal sources via weathering processes.

(6) The positive Ce and La anomalies indicate both terrigenous input and contribution of the oxidative compounds from sulfide-rich mineralization in the Euphrates River bed sediments.

(7) The chondrite, NAS, and UCC normalized patterns show that the REE compositions of the Euphrates River sediments differ from chondrite but are similar to NAS and UCC.

(8) The Sm and Eu patterns are close to 1, and Gd pattern is higher than 1 (>1), and also $Gd/Yb_{NAS\ and\ UCC}$ ratio greater than 1 indicates that the source of REE may be apatite-rich granodioritic rocks which are from the Elazığ Magmatic Complex. Also, terrigenous sediments and lithological control are more effective on the Euphrates River sediment REE compositions.

(9) The Euphrates River waters have the highest composition values for both LREE and HREE in comparison to the other basic river waters (the Amazon, Indus, Ohio, and

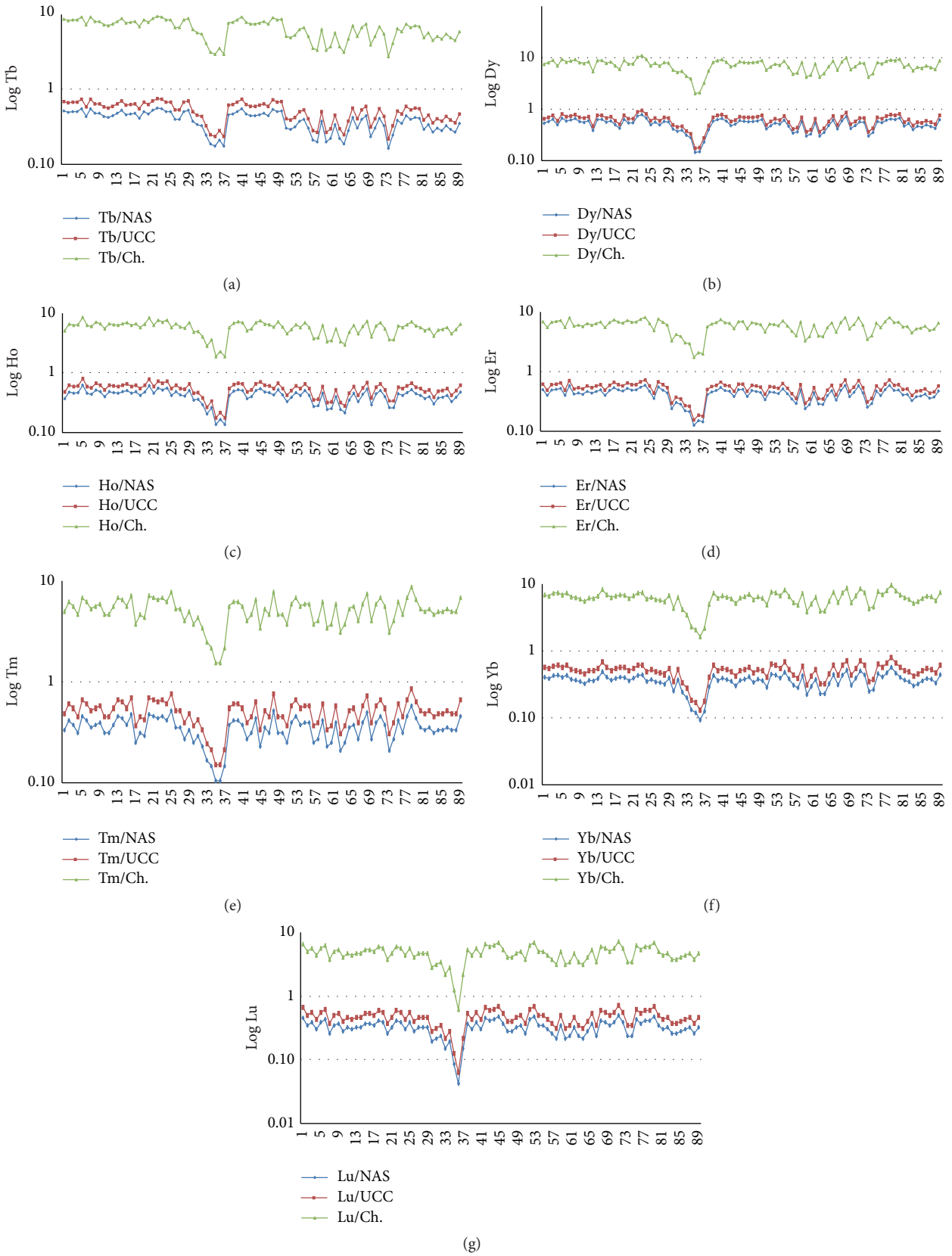

Figure 4: Normalized patterns of the HREE average concentrations ($N = 90$) of Euphrates River sediments in the NAS, UCC, and Ch. (a) Tb, (b) Dy, (c) Ho, (d) Er, (e) Tm, (f) Yb, and (g) Lu normalized patterns.

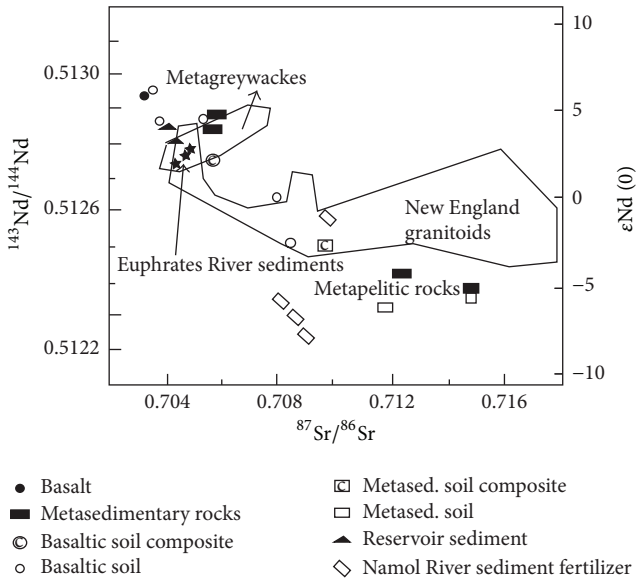

Figure 5: Diagram of Nd versus Sr isotopic composition in rock, soil, and sediment samples from Martin and McCulloch [4]. Lines connect rock and soil samples taken from the same locality. Outlined fields show isotopic compositions of the New England granitoids, metapelitic rocks, and metagraywackes from the New England fold belt [49].

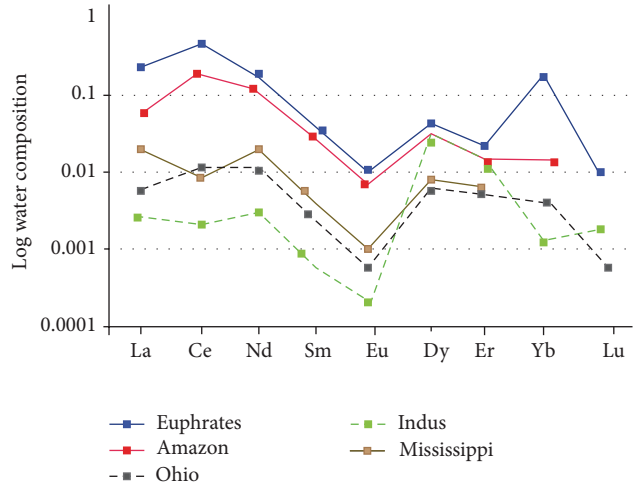

Figure 6: Distribution of REE in the Euphrates River waters and the Amazon, Indus, Mississippi, and Ohio River waters data from Goldstein and Jacobsen [13].

Mississippi River waters) due to regional felsic and mafic lithological units. Due to circulation of mixing water, REE concentrations increase in the river water but decrease in the river sediments.

Competing Interests

The authors declare that there are no competing interests regarding the publication of this paper.

Acknowledgments

The authors would like to thank FUBAP for the research support (Project no. MF 14.26).

References

[1] W. H. Burke, R. E. Denison, E. A. Hetherington, R. B. Koepnick, H. F. Nelson, and J. B. Otto, "Variation of seawater $^{87}Sr/^{86}Sr$ throughout Phanerozoic time," *Geology*, vol. 10, no. 10, pp. 516–519, 1982.

[2] J. F. V. R. Bussy, "Pétrogenèse des enclaves microgrenues associées aux granitoides calco-alcalins: exemple des massifs varisque du Mont-Blanc (Alpes occidentales) et Miocène du Monte Capanne (Ile d'Elbe, Italie)," *Mémoires de Géologie (Lausanne)*, vol. 7, p. 309, 1990.

[3] F. X. Gingele and P. De Deckker, "Late Quaternary fluctuations of palaeoproductivity in the Murray Canyons area, South Australian continental margin," *Palaeogeography, Palaeoclimatology, Palaeoecology*, vol. 220, no. 3-4, pp. 361–373, 2005.

[4] C. E. Martin and M. T. McCulloch, "Nd-Sr isotopic and trace element geochemistry of river sediments and soils in a fertilized catchment, New South Wales, Australia," *Geochimica et Cosmochimica Acta*, vol. 63, no. 2, pp. 287–305, 1999.

[5] M. Revel-Rolland, F. Arnaud, E. Chapron et al., "Sr and Nd isotopes as tracers of clastic sources in Lake Le Bourget sediment (NW Alps, France) during the Little Ice Age: palaeohydrology implications," *Chemical Geology*, vol. 224, no. 4, pp. 183–200, 2005.

[6] R. L. Cullers, T. Barrett, R. Carlson, and B. Robinson, "Rare-earth element and mineralogic changes in Holocene soil and stream sediment: a case study in the Wet Mountains, Colorado, U.S.A.," *Chemical Geology*, vol. 63, no. 3-4, pp. 275–297, 1987.

[7] W. Zhu, M. Kennedy, E. W. B. de Leer, H. Zhou, and G. J. F. R. Alaerts, "Distribution and modelling of rare earth elements in Chinese river sediments," *Science of the Total Environment*, vol. 204, no. 3, pp. 233–243, 1997.

[8] S. Y. Yang, H. S. Jung, M. S. Choi, and C. X. Li, "The rare earth element compositions of the Changjiang (Yangtze) and Huanghe (Yellow) river sediments," *Earth and Planetary Science Letters*, vol. 201, no. 2, pp. 407–419, 2002.

[9] H. W. Nesbitt, "Mobility and fractionation of rare earth elements during weathering of a granodiorite," *Nature*, vol. 279, pp. 206–210, 1979.

[10] J.-J. Braun, J. Viers, B. Dupré, M. Polve, J. Ndam, and J.-P. Muller, "Solid/liquid REE fractionation in the lateritic system of Goyoum, East Cameroon: the implication for the present dynamics of the soil covers of the humid tropical regions," *Geochimica et Cosmochimica Acta*, vol. 62, no. 2, pp. 273–299, 1998.

[11] B. Rasmussen and J. E. Glover, "Diagenesis of low-mobility elements (Ti, REEs, Th) and solid bitumen envelopes in Permian Kennedy Group sandstone, western Australia," *Journal of Sedimentary Research*, vol. 64, pp. 572–583, 1994.

[12] R. H. Meade and R. S. Parker, "Sediment in the rivers of the United State," in *U.S. Geological Survey, Water Supply Paper*, vol. 2275, pp. 49–60, 1985.

[13] S. J. Goldstein and S. B. Jacobsen, "Rare earth elements in river waters," *Earth and Planetary Science Letters*, vol. 89, no. 1, pp. 35–47, 1988.

[14] D. G. Brookins, "Aqueous geochemistry of rare earth elements," in *Geochemistry and Mineralogy of Rare Earth Elements*, B. R.

Lipin and G. A. McKay, Eds., vol. 21, chapter 8, pp. 201–226, Mineralogical Society of America, 1989.

[15] H. Elderfield, R. Upstill-Goddard, and E. R. Sholkovitz, "The rare earth elements in rivers, estuaries, and coastal seas and their significance to the composition of ocean waters," *Geochimica et Cosmochimica Acta*, vol. 54, no. 4, pp. 971–991, 1990.

[16] K. H. Johannesson, D. L. Hawkins Jr., and A. Cortés, "Do Archean chemical sediments record ancient seawater rare earth element patterns?" *Geochimica et Cosmochimica Acta*, vol. 70, no. 4, pp. 871–890, 2006.

[17] I. Hossain, K. K. Roy, P. K. Biswas, M. Alam, M. Moniruzzaman, and F. Deeba, "Geochemical characteristics of Holocene sediments from Chuadanga district, Bangladesh: implications for weathering, climate, redox conditions, provenance and tectonic setting," *Chinese Journal of Geochemistry*, vol. 33, no. 4, pp. 336–350, 2014.

[18] S. O. Obaje, I. A. Akpoborie, F. C. Ugbe, and A. Onugba, "Rare earth and trace elements distribution in sediments of River Gora, Minna Area, North-Central Nigeria: implication for provenance," *Earth Science Research* , vol. 4, no. 1, pp. 103–112, 2015.

[19] M. I. Leybourne, W. D. Goodfellow, D. R. Boyle, and G. M. Hall, "Rapid development of negative Ce anomalies in surface waters and contrasting REE patterns in groundwaters associated with Zn-Pb massive sulphide deposits," *Applied Geochemistry*, vol. 15, no. 6, pp. 695–723, 2000.

[20] L. Kalender and L. Bölücek, "Major and trace elemet contamination of groundwaters, stream sediments and plants of the abandoned mines in Keban district (Elazığ) of Eastern Anatolia, Turkey," in *Proceedings of the 57th Geological Congress of Turkey*, p. 187, MTA Culture Sites, Ankara, Turkey, March 2004.

[21] L. Kalender and S. Çiçek Uçar, "Assessment of metal contamination in sediments in the tributaries of the Euphrates River, using pollution indices and the determination of the pollution source," *Turkey Journal of Geochemical Exploration*, vol. 134, pp. 73–84, 2013.

[22] K. C. Condie, "Another look at REEs in shales," *Geochimica et Cosmochimica Acta*, vol. 55, no. 9, pp. 2527–2531, 1991.

[23] S. R. Taylor, S. M. McLennan, R. L. Armstrong, and J. Tarney, "The composition and evolution of the continental crust: rare earth element evidence from sedimentary rocks," *Philosophical Transactions of the Royal Society A: Mathematical, Physical and Engineering Sciences*, vol. 301, no. 1461, pp. 381–399, 1981.

[24] S. R. Taylor, S. M. McLennan, and M. T. McCulloch, "Geochemistry of loess, continental crustal composition and crustal model ages," *Geochimica et Cosmochimica Acta*, vol. 47, no. 11, pp. 1897–1905, 1983.

[25] S. R. Taylor, *Solar System Evolution*, Cambridge University Press, Cambridge, UK, 1992.

[26] E. Herece, E. Akay, Ö. Küçümen, and M. Sarıaslan, "Geology of Elazığ-Sivrice-Palu area," Report MTA 9634, 1992.

[27] K. Frenken, "Irrigation in the Middle East region in figures," Water Reports 34, FAO, Rome, Italy, 2009, AQUASTAT Survey 2008.

[28] L. Kalender and Ş. Hanelçi, "General features of copper mineralization in the eastern Euphrates, Keban-Elazığ area, Turkey," *Journal Geological Society of India*, vol. 64, pp. 655–665, 2004.

[29] M. Turan, E. Aksoy, and A. F. Bingöl, "The characterizations of the east Taurus geodynamic evolution in the Elazig area," in *Proceedings of the Symposium for the 25th Anniversary of Earth Sciences at Hacettepe University*, Ankara, Turkey, November 1993.

[30] M. Beyarslan and F. Bingöl, "Ultramafics and mafic bodies in cumulates of ispendere and kömürhan ophiolites (SE Anatolian Belt. Turkey)," *Turkish Journal of Science and Technology*, vol. 51, no. 1, pp. 19–36, 2010.

[31] M. Turan, E. Aksoy, and A. F. Bingöl, "The characterizations of the east Taurus geodynamic evolution in the Elazig area," *University of Firat, Sciences and Engineering Bulletin*, vol. 72, pp. 1–23, 1995 (abstract in Engilish).

[32] İ. Türkmen, M. İnceöz, E. Aksoy, and M. Kaya, "New findings on Eocene stratigraphy and paleogeography of Elazğ area," *Bulletin of the Earth Sciences Application and Research Centre of Hacettepe University*, vol. 24, pp. 81–95, 2001.

[33] D. Perinçek and H. Kozlu, "Stratigraphy and structural relation of the units in the Afşin-Elbistan-Doğanşehir Region," in *Proceedings of the International Symposium on the Geology of the Taurus Belt*, O. Tekeli and C. Göncüoğlu, Eds., pp. 181–198, Mineral Research & Exploration Institute, Ankara, Turkey, 1984.

[34] O. Sungurlu, D. Perinçek, G. Kut et al., "Geology of the Elazığ, Hazar and Palu area," *The General Directorate of Petroleum Affairs*, vol. 29, pp. 83–191, 1985 (Turkish).

[35] Y. Yılmaz, E. Yiğitbaş, and Ş. C. Genç, "Ophiolitic and metamorphic assemblages of Southeast Anatolia and their significance in the geological evolution of the orogenic belt," *Tectonics*, vol. 12, no. 5, pp. 1280–1297, 1993.

[36] M. Turan and A. F. Bingöl, "Tectono-stratigraphic characterizations of between Kovancılar and Baskil (Elazığ) area," in *Proceedings of the Ahmet Acar Geology Symposium, Cukurova University*, pp. 213–217, Adana, Turkey, 1991 (Turkish).

[37] İ. Türkmen, E. Aksoy, S. Kürüm, B. Akgül, and M. İnceöz, "Lower Miocene volcanism of Arguvan-Arapgir (Malatya) region and their significance in the regional stratigraphy," *Geosound*, vol. 32, pp. 103–115, 1998 (abstract in English).

[38] İ. Türkmen, "Stratigraphy and sedimentological features of Çaybağı Formation (Upper Miocene-Pliocene?) in the eastern Elaziğ," *Bulletin of Turkish Geological Society*, vol. 34, no. 5, pp. 45–53, 1991.

[39] E. Kerey and İ. Türkmen, "Sedimentological aspects of Palu Formation (Pliocene-Quaternary), The east of Elazığ, Turkey," *Geological Bulletin of Turkey*, vol. 34, pp. 21–26, 1991.

[40] F. Ackermann, "A procedure for correcting the grain size effect in heavy metal analyses of estuarine and coastal sediments," *Environmental Technology Letters*, vol. 1, no. 11, pp. 518–527, 1980.

[41] L. Kalender and C. Bölücek, "Environmental impact and drainage geochemistry in the vicinity of the Harput Pb-Zn-Cu veins, Elazığ, SE Turkey," *Turkish Journal of Eath Sciences*, vol. 16, pp. 241–255, 2007.

[42] S. Saito, O. Ohno, S. Igarashi, T. Kato, and H. Yamaguchi, "Separation and recycling for rare earth elements by homogeneous liquid-liquid extraction (HoLLE) using a pH-responsive fluorine-based surfactant," *Metals*, vol. 5, no. 3, pp. 1543–1552, 2015.

[43] S. Köksal and M. C. Göncüoğlu, "Sr and Nd isotopic characteristics of some S, I and a type granitoids from central anatolia," *Turkish Journal of Earth Sciences*, vol. 17, pp. 111–127, 2008.

[44] I. Raczek, K. P. Jochum, and A. W. Hofmann, "Neodymium and strontium isotope data for USGS reference materials BCR-1, BCR-2, BHVO-1, BHVO-2, AGV-1, AGV-2, GSP-1, GSP-2 and eight MPI-DING reference glasses, Geostandards Newsletter," *The Journal of Geostandards and Geoanalysis*, vol. 27, pp. 173–179, 2003.

[45] C. K. Gupta and N. Krishnamurthy, *Metallurgy of Rare Earths*, CRC Press, 2005.

[46] E. R. Sholkovitz, "The aquatic chemistry of rare earth elements in rivers and estuaries," *Aquatic Geochemistry*, vol. 1, no. 1, pp. 1–34, 1995.

[47] B. Akgül, M. Akgül, M. Satır, and A. Sağıroğlu, "Geochronology and ısotope geochemistry of the Upper CretaceousElazığ Magmatites in Eastern Anatolia (Turkey): implications for petrogenesis and tectonic evolution," in *Proceedings of the 45th Anniversary Geology Symposium*, p. 21, Trabzon, Turkey, October 2010.

[48] H. D. Mensel, M. T. McCulloch, and B. W. Chappell, "The New England Batholith: constraints on its derivation from Nd and Sr isotopic studies of granitoids and country rocks," *Geochimica et Cosmochimica Acta*, vol. 49, no. 2, pp. 369–384, 1985.

[49] W. F. McDonough, M. T. McCulloch, and S. S. Sun, "Isotopic and geochemical systematics in Tertiary-Recent basalts from southeastern Australia and implications for the evolution of the sub-continental lithosphere," *Geochimica et Cosmochimica Acta*, vol. 49, no. 10, pp. 2051–2067, 1985.

[50] E. R. Sholkovitz, "Rare earth elements in the sediments of the North Atlantic Ocean, Amazon Delta, and East China Sea: reinterpretation of terrigenous input patterns to the oceans," *American Journal of Science*, vol. 288, no. 3, pp. 236–281, 1988.

[51] E. R. Sholkovitz, "Chemical evolution of rare earth elements: fractionation between colloidal and solution phases of filtered river water," *Earth and Planetary Science Letters*, vol. 114, no. 1, pp. 77–84, 1992.

[52] J. F. Banfield and R. A. Eggleton, "Apatite replacement and rare earth mobilization, fractionation, and fixation during weathering," *Clays & Clay Minerals*, vol. 37, no. 2, pp. 113–127, 1989.

[53] R. E. Hannigan and E. R. Sholkovitz, "The development of middle rare earth element enrichments in freshwaters: weathering of phosphate minerals," *Chemical Geology*, vol. 175, no. 3-4, pp. 495–508, 2001.

[54] R. Ramesh, A. Ramanathan, S. Ramesh, R. Purvaja, and V. Subramanian, "Distribution of rare earth elements and heavy metals in the surficial sediments of the Himalayan river system," *Geochemical Journal*, vol. 34, no. 4, pp. 295–319, 2000.

[55] S. G. Nielsen, C. T. A. Lee Shimizu, and N. M. Behn, "The sulfur abundance of the mantle deduced from trace element ratios," in *Proceedings of the 24th Goldschmidt Meeting*, p. 1814, Sacramento, Calif, USA, June 2014.

[56] J. Luo, Y. Hu, Y. Shen, J. Hu, and H. Ji, "Effects of colloidal particle size on the geochemical characteristics of REE in the water in southern Jiangxi province, China," *Environmental Earth Sciences*, vol. 75, no. 1, article 81, 17 pages, 2016.

[57] G. N. Hanson, "Rare earth elements in petrogenetic studies of igneous systems," *Annual Review of Earth and Planetary Sciences*, vol. 8, no. 1, pp. 371–406, 1980.

[58] L. P. Gromet and L. T. Silver, "Rare earth element distributions among minerals in a granodiorite and their petrogenetic implications," *Geochimica et Cosmochimica Acta*, vol. 47, no. 5, pp. 925–939, 1983.

[59] J. Hermann, "Allanite: thorium and light rare earth element carrier in subducted crust," *Chemical Geology*, vol. 192, no. 3-4, pp. 289–306, 2002.

[60] M. I. Leybourne and K. H. Johannesson, "Rare earth elements (REE) and yttrium in stream waters, stream sediments, and Fe–Mn oxyhydroxides: fractionation, speciation, and controls over REE + Y patterns in the surface environment," *Geochimica et Cosmochimica Acta*, vol. 72, no. 24, pp. 5962–5983, 2008.

[61] M. Mishra and S. Sen, "Provenance, tectonic setting and source-area weathering of Mesoproterozoic Kaimur Group, Vindhyan Supergroup, Central India," *Geologica Acta*, vol. 10, no. 3, pp. 243–253, 2012.

[62] E. D. Goldberg, M. Koide, R. A. Schmitt, and R. H. Smith, "Rare-earth distributions in the marine environment," *Journal of Geophysical Research*, vol. 68, no. 14, pp. 4209–4217, 1963.